FEL OSCILLATION WITH A HIGH EXTRACTION EFFICIENCY AT JAEA ERL FEL

N. Nishimori*, R. Hajima, H. Iijima, N. Kikuzawa, E. Minehara, R. Nagai, T. Nishitani, M. Sawamura, JAEA, Ibaraki, Japan.

Abstract

One of challenges that high-power FEL oscillators driven by energy recovery linac (ERL) are facing is to increase the extraction FEL efficiency as high as possible. The high-efficiency oscillation relaxes the total beam current needed for high-power lasing and makes the optical micropulse length shorter, which is useful for various applications. Two triple bend achromatic arcs have been used in a recovery loop for an ERL FEL at Japan Atomic Energy Agency (JAEA). The return arc after an undulator has an energy acceptance of 15%, which is large enough to recover the electron beam used for high-efficiency FEL oscillation. Recently we have achieved the efficiency exceeding 2%, which accompanies large energy spread, by doubling the electron bunch repetition rate. The FEL efficiency has been measured from the horizontal profiles of the exhausted electron beam with a wire scanner installed at a dispersive point in the return arc. The other arc placed upstream of the undulator has been found to work as a bunch compressor for the high-efficiency FEL oscillation.

INTRODUCTION

One of challenges that high-power FEL oscillators driven by energy recovery linac (ERL) are facing is to increase the extraction FEL efficiency as high as possible. The high-efficiency oscillation saves the total beam current needed for high-power lasing, which decreases the beam load to various accelerator components and increases the wall-plug efficiency. The high-efficiency oscillation is also appropriate for producing broadband ultrashort optical pulses, and makes the optical micropulse length shorter, which is useful for various applications [1].

In a high-power ERL FEL at Jefferson Lab, a high-efficiency FEL oscillation has been achieved at near IR wavelength region [2, 3, 4]. The exhausted beam is transported to accelerators through a Bates type recovery loop with energy acceptance of 15%, and full energy recovery has been successfully established [5]. A recovery loop which consists of two triple bend achromatic arcs has been used for an ERL FEL at Japan Atomic Energy Agency (JAEA) [6]. The energy acceptance of the return arc after an undulator was 7% before June 2006 [7, 6]. Recently we have achieved the efficiency exceeding 2%, which accompanies large energy spread beyond the energy acceptance of the arc, by doubling the electron bunch repetition rate [8]. The optical pulse can now interact with a fresh electron bunch every round trip, while it overlapped with an injected electron bunch every two round trips before the doubling.

In this paper, first we give brief description of the configuration and recent upgrade of JAEA ERL for a high-power FEL oscillation with the doubled beam current. Then our recent experimental results on the FEL efficiency and the beam dynamics through the energy recovery loop are reported in details. The FEL efficiency has been measured with a wire scanner installed at a dispersive point in the return arc, which can serve as a monitor of the energy distribution of the exhausted electron beam. The wire scanners have been also installed at other dispersive points for study of the beam dynamics through the triple bend achromatic arcs. A measurement of the energy distributions at the first arc, which is placed upstream of the undulator, as a function of the accelerator phase has revealed that magnetic bunch compression in the first arc is indispensable for a high-power FEL oscillation at the JAEA ERL. Finally, applications planned in JAEA FEL are presented.

CONFIGURATION OF JAEA ERL

The JAEA FEL facility has been developed as a high-power FEL at wavelength in far infrared region around 20 μm. The laser output power exceeded 1 kW within 500 μs macropulse duration without energy-recovery in 2000 [9]. In order to increase the FEL output power higher than 10 kW and demonstrate the technology and commercial profit of high-power FELs for industrial applications, we have developed an ERL FEL as an extension of the original superconducting accelerator [10].

The layout of the JAEA ERL is shown in Fig. 1. An injector, main super-conducting accelerator (SCA) modules, an undulator, and the first arc are from the original FEL. An injection merger, a half chicane before the undulator, and the return arc were installed for the ERL. The injector consists of 230 kV electron gun with a thermionic cathode, 83.3 MHz subharmonic buncher (SHB), and two cryomodules, each of which has a single cell SCA cavity driven at 499.8 MHz. An electron bunch of 0.5 nC with full width half maximum (FWHM) length of 600 ps is generated by a grid pulser at a 10.4 MHz repetition rate, that is 5 mA average current, and compressed by the SHB followed by a 4.5-m drift. The electron bunch is accelerated to 2.5 MeV by two single cells, and further compressed by ballistic bunching through a 9-m drift. A two-step staircase is used for the injection merger, because this configuration fulfills the design requirements, achromaticity and small emittance

* nishimori.nobuyuki@jaea.go.jp

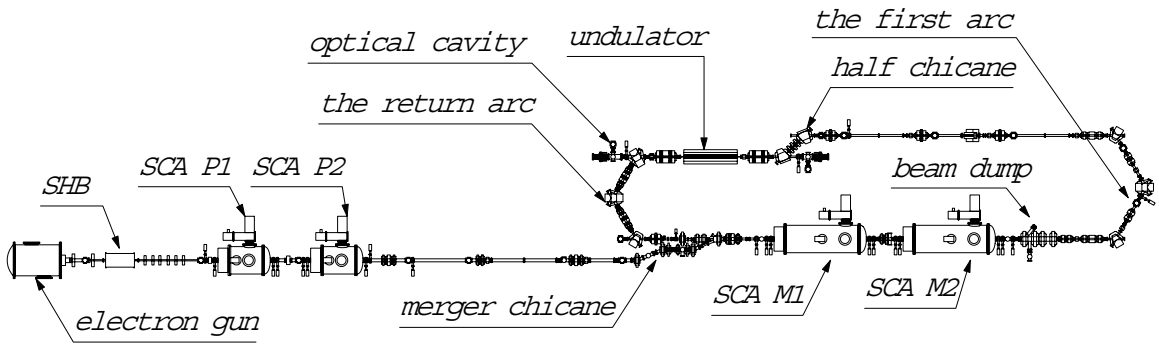

Figure 1: The layout of JAEA Energy-Recovery Linac. An electron bunch generated by 230 kV electron gun is accelerated to 2.5 MeV and injected into the energy-recovery loop. The electron bunch is accelerated to 17 MeV by main superconducting cavities and transported to the FEL undulator. The electron bunch is, then, re-injected to the main cavities and decelerated down to 2.5 MeV and collected by a beam dump.

growth, and fits in the existing space. The achromaticity of the merger is realized by setting three quadrupole magnets to the appropriate strengths. An electron bunch injected to two main cryomodules, each of which has five cell SCA cavities driven at 499.8 MHz, is accelerated up to 17 MeV and transported to the undulator through the first arc and the half chicane. After the FEL interaction, the electron bunch is re-injected into the main cryomodules at a deceleration phase for the energy recovery. The re-injection phase can be controlled by changing the recirculation path length. The return arc has been placed on movable tables for this purpose. Both arcs used in the recirculation loop have two families of quadrupole magnets which enable one to vary M_{56} while maintaining achromaticity. This variable M_{56} can be used for bunch compression in the first arc and for energy compression in the return arc. The return arc also has two families of sextupole magnets to compensate second-order aberrations T_{166}, T_{266}, T_{566} arising from the large energy spread due to the FEL interaction.

The JAEA ERL-FEL has been operated in pulsed mode of 1 ms macropulse length in maximum and 10 Hz repetition rate, because of the following reasons. 1) The cooling power of the refrigerator system for the SCA modules is not sufficient enough to operate in CW mode. 2) The shield of the building for the linac is not thick enough for the radiation protection.

UPGRADE OF JAEA ERL

Gun Grid Pulser and Injector RF sources

Increasing the injector beam current is a straightforward approach to increase the FEL power by taking full advantage of the energy-recovery. The JAEA gun has a thermionic cathode driven by a grid pulser. In the original configuration, the gun was designed to produce 0.5 nC electron bunches at 10.4 MHz repetition. We installed a new grid pulser working at 20.8 MHz, doubled repetition of the original one, and a 10 mA beam is now available [11]. The new grid pulser is designed at Budker Institute of Nuclear Physics and can be operated in CW-mode as well as pulsed mode [12]. The electron beam properties with the new grid pulser keep similar performance to the original one. The pulse width and the normalized rms emittance at the gun are 590 ps (FWHM) and 20 πmm·mrad, respectively [11].

Two single-cell cavities of the injector were driven by 8 kW solid state amplifier for each, enough capacity for 5 mA operation. The solid state amplifier was replaced by an IOT-klystrode of 50 kW, which enables one to inject a 40 mA beam into the ERL [13].

RF low-level controllers

Stable operation of an FEL relies much on the stability of an accelerator. An RF low-level controller for a SCA is one of the key components for achieving good stability. The original JAEA FEL was equipped with a low-level controller, which kept phase flatness at ± 1 degree within a 1 ms macropulse. The low-level controller was replaced by new one, which provides the following functions for the better stability: the feedback gain and bandwidth can be varied during operation to obtain good flatness of RF phase and amplitude, and all the circuits are contained in boxes with temperature stabilization. The new controller is installed in the vicinity of the SCA cavity to make the cable length between the controller and the SCA as short as possible. Furthermore the cables between the controller and the cavities are contained in a temperature-controlled pipe to suppress the temperature drift. After these upgrade, the accuracy and stability of accelerating RF has been improved. The flatness of RF phase and amplitude within a 1 ms macropulse are 0.06 deg. rms and 0.013% rms, respectively, while those for the old system were 0.20 deg. and 0.013% [14]. Phase and amplitude fluctuations for 5 minutes in the new system are measured as 0.15 deg. and

0.015%, respectively.

Increased energy acceptance of the arcs

The doubled beam current has enabled us to operate the JAEA ERL FEL with efficiency higher than 2%. The resulting large energy spread of the exhausted electron beam exceeded the energy acceptance of the return arc, which caused a radiation problem when the FEL was operated for a long time period at a macropulse length longer than 250 μs. We made minor modification of the return arc to increase the beam energy acceptance. The bore of quadrupole magnets of the return arc was enlarged from 64 mm to 102 mm. The beam pipe diameter was enlarged from 55 mm to 100 mm. The energy acceptance of the return arc has been increased from 7% to 15%. The quadrupole magnets in the first arc were also replaced with those used in the return arc. The energy acceptance of the first arc has been increased from 3.5% to 4.3%.

FEL EFFICIENCY

The FEL wavelength at the JAEA FEL is around 20 μm and a holed mirror is used to couple FEL out of the optical cavity. The coupling efficiency of the holed mirror is estimated to be around 30% [15]. It is however difficult to exactly determine the FEL efficiency from the measured FEL power only. The FEL efficiency can be obtained from a measurement of the beam centroid shift of the exhausted beam from the position without lasing at a dispersive point. A non-destructive method is indispensable for the energy analyzer, since the exhausted beam has to be recovered under an ERL operation. A synchrotron radiation (SR) monitor allows for continuous monitoring of the energy spectrum of the beam for an ERL operated even at a full power [16, 5]. The SR wavelength at the JAEA ERL is however longer than 20 μm, where no monitor camera is available. A beam position monitor is also a promising candidate for measuring the shift of the beam centroid [17]. It does not however provide information about the energy distribution of the exhausted beam, which is also important for beam energy recovery. We decided to use a wire scanner, which is appropriate for measuring profiles of pulsed or low-current-CW beams, although it is a partially intercepting device.

Wire Scanners

A wire scanner consists of a thin wire that is moved across the beam path. The local density of the electrons traversing the wire is detected by measuring such secondary particles as secondary electrons and bremsstrahlung photons produced by the interaction of the electron beam with the wire. Detection of the secondary particles allows one to measure the beam profile, and wire scanners are widely used as beam profile monitors. Detecting bremsstrahlung photons with a scintillator and a photomultiplier placed downstream of the wire has enabled one to measure large dynamic range beam profile in an ERL where small beam loss like beam halo represents significant amount of beam power [18]. A wire array based on secondary electron emission current is used to provide time resolved electron spectrum, which is useful to study the evolution of the energy spectrum from a narrow to a broad spectrum as a result of the FEL interaction [19, 20].

The wire scanner used in the present study is based on a linear movement of a copper wire in 0.6 mm diameter through the beam at a speed of 0.39 mm/s by 100 mm-stroke. The copper wire is mounted on an aluminium fork with a gap of 26 mm and electrically floated from the ground. The secondary electron emission current is measured with a current meter (TR8641 electronic picoammeter, ADVANTEST). The wire position is measured with a linear potentiometer and is recorded in an ADC (WE7272 isolated digitizer, YOKOGAWA) together with the secondary electron current.

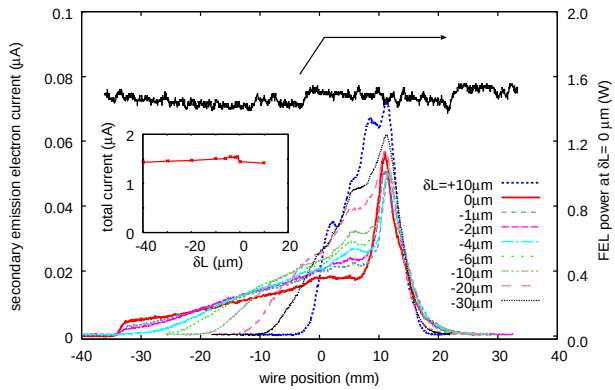

Figure 2: Horizontal beam profiles for various cavity detuning lengths measured with a wire scanner (WIRE #1) placed in the middle of the drift space between two quadrupole magnets just after the first bending magnet in the return arc, where horizontal dispersion is measured to be η = 0.376 m. The vertical axis shows secondary electron emission current and horizontal axis shows wire position. The total secondary emission electron current integrated along the wire position is plotted with respect to optical cavity detuning length in the inset. The FEL power at δL = 0 μm during a wire scan is represented by a black solid line.

Electron energy distributions and FEL efficiency

Figure 2 shows horizontal beam profiles measured for various detuning lengths (δLs) of an optical cavity with the wire scanner, which is installed in the middle between two quadrupole magnets placed just after the first bending magnet in the return arc. This wire is called WIRE #1 in the present paper. The horizontal dispersion at the wire scanner is measured to be η = 0.376 m from the shift of the beam centroid with respect to the magnetic field of the first bending magnet. This is similar to the value of η =

0.41 m calculated from a first-order matrix of beam transport (see Fig. 5). The vertical axis shows secondary emission electron current from the wire scanner and horizontal axis shows wire position. The polarity of the secondary electron current is positive. The inset shows the total secondary emission current integrated along the wire position as a function of δL. The total secondary current is 1.5 μA, which is almost independent of δL. The secondary electron production rate for 17 MeV electron on our wire scanner is estimated to be 8%, since the incident electron beam current during the measurement was 18.5 μA. The production rate is similar to that for for 30 MeV electron on carbon, which is measured to be 3% [21]. The peak secondary electron current measured by the wire is less than 0.07 μA (see Fig. 2), indicating that the beam loss due to the presence of the wire is small (less than 5%). This explains our observation that the FEL power at δL = 0 μm remains unchanged during the wire scan, which is shown by a black solid line in Fig. 2,

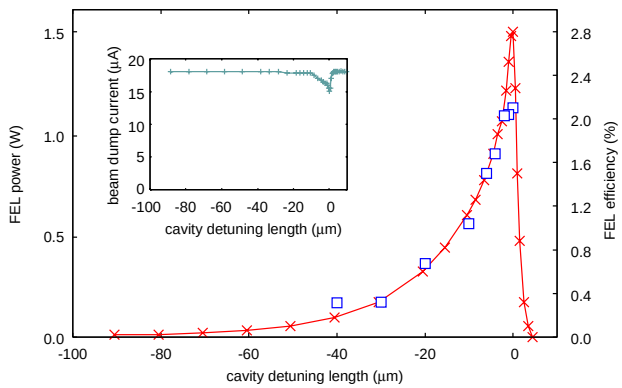

Figure 3: FEL power measured as a function of δL at macropulse length of 230 μs. FEL efficiencies obtained from the energy distributions of the exhausted electron beam are shown by open squares. The efficiencies near zero detuning length cannot be measured with our energy analyzer due to the limited energy acceptance, and they are determined from measured FEL power. The inset shows the beam dump current with respect to δL.

The FEL power changes as a function of δL, as shown in Fig. 3, and the energy distributions of the exhausted electron beam changes as well (see Fig. 2). The shift of the beam centroid from the position without lasing yields the FEL efficiency together with the dispersion η = 0.376 m. The measured FEL efficiencies are plotted as open squares in Fig. 3. The efficiency higher than 2% cannot be measured with our present wire scanner, since the scanner is placed downstream of the focusing quadrupole magnet where the dispersion is maximum of η = 0.6 m. The sharp edge of the beam profiles seen around the wire position of -34 mm in Fig. 2 represents the beam loss in the lower energy side at the first quadrupole. The amount of the beam loss is considered to be small, since the total secondary electron current is almost constant with respect to δL (see inset of Fig. 2). The maximum FEL efficiency is estimated to be 2.8%, as shown in Fig. 3.

Table 1: JAEA ERL FEL parameters

Parameter	Measured
Beam energy at undulator	17 MeV
Average current at undulator	8 mA
Bunch charge at undulator	0.4 nC
Bunch length at undulator	12 ps (FWHM)
Peak current	35 A
Energy spread before undulator	1.5% (FWHM)
after undulator	$>$ 15% (full)
Normalized emittance (rms)	40 mm mr
Bunch repetition	20.8250 MHz
Macropulse	1 ms $\times$ 10 Hz
Undulator period	3.3 cm
Number of undulator periods	52
Undulator parameter (rms)	0.7
Optical cavity length	7.2 m
Rayleigh range	1.00 m
Mirror radii	6 cm
Output wavelength	22 μm
FEL extraction efficiency	$>$ 2.5%

The coupling efficiency of the holed mirror is obtained from the present efficiency measurement. The measured FEL power is 1.5 W for macropulse length of 230 μs. The FEL power during the macropulse is estimated to be 0.75 kW, since the FEL power for the first 30 μs is negligibly small. The FEL is extracted through a KRS5 window, that has the transmittance of 70% in normal incidence. The beam current measured at the beam dump is 18.5 μA corresponding to the average beam current of 8 mA. From those experimental results, the coupling efficiency of the holed mirror is estimated to be 28% and agrees well with the calculated value of 30% [15]. The JAEA ERL FEL parameters are listed in Table 1.

Thermal effect on the wire scanner

Heating of the wire might be a concern when attempting to measure the profile of high average power electron beams [22]. The stopping power for 17 MeV electrons in copper is 2.5 MeV cm^2/g. [23], and the specific gravity of copper is 8.94 g/cm^3. We assume that the copper wire in 0.6 mm diameter is regarded as a foil with width of 0.532 mm and depth of 0.532 mm. The energy loss of 17 MeV electron in the copper wire is estimated to be 1.2 MeV. The total charge struck by the electron beam during a wire scan is measured to be less than 25 μC when macropulse length is 230 μs, and the maximum power deposited on the wire during the scan is 30 J. The specific heat of copper is 0.385 J/g/K at 25°C. Thus the temperature rise of the wire can be estimated to be 15000 K in maximum when we assume that the heat accumulates in the wire within a vertical distance of 2 mm, which is similar to the vertical beam size.

However we need to take thermal radiation power, thermal conductivity of copper, power of secondary emission particles, and others which can alleviate the temperature rise of the wire, into account. Although the wire scanner can be used as an energy analyzer as long as heating is not a problem, we need to study this thermal effect in details.

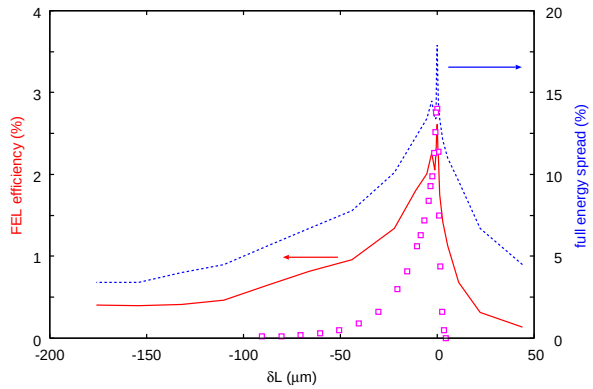

Figure 4: FEL efficiencies as a function of δL obtained from a one-dimensional time-dependent FEL simulation (solid line) and corresponding beam energy spread (dotted line). Measured FEL efficiencies are also plotted as open squares for comparison.

FEL simulation

We have conducted an FEL simulation for comparison with the experimental result. We use one-dimensional time-dependent FEL simulation code, which was used in our previous studies [24] and agrees well with experimental results obtained without energy recovery. The electron bunch length measured at the undulator center is 12 ps (FWHM). The electron bunch shape used in the simulation is assumed to be triangular with the peak Colson's dimensionless beam current of j_0 = 25. A mono energetic electron beam is assumed in the simulation, since the peak FEL efficiency depends little on initial energy spread [24]. The optical cavity loss is measured to be 4.2% from a cavity ring down of the FEL pulse with a Ge:Cu detector. Figure 4 shows calculated FEL efficiency and full energy spread of an electron bunch as a function of δL. The measured FEL efficiencies are much smaller than those obtained in the simulation at large detuning lengths. This may be due to the large energy spread of the incident electron beam.

BEAM TRANSPORT IN THE RETURN ARC

Transverse and longitudinal beam dynamics through the return arc for JAEA ERL has been already studied to find a matched beam envelope from the undulator to the beam dump [7]. In order to roughly estimate dispersion and M_{56} in the return arc, we calculate the beam envelope

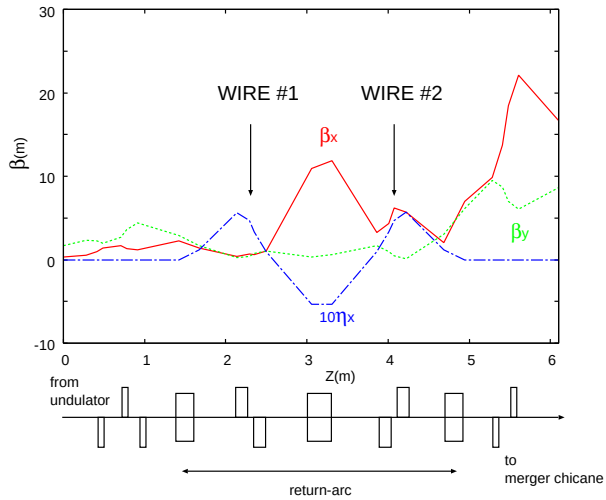

Figure 5: Beam envelopes from the undulator exit through the return arc to the merger chicane calculated from a first-order matrix of beam transport. The positions of wire scanners are indicated by arrows.

from the undulator to the entrance of main SCA modules based on magnet parameters used for actual beam transport. Courant-Snyder parameters at the exit of the undulator are given from the matched beam condition for the undulator, α_x = 0; β_x = 0.33 m; α_y =−1; β_y = 1.7 m. Figure 5 shows obtained betatron functions for the beam envelope, where M_{56} = −0.56 m from the undulator to the entrance of the merger chicane.

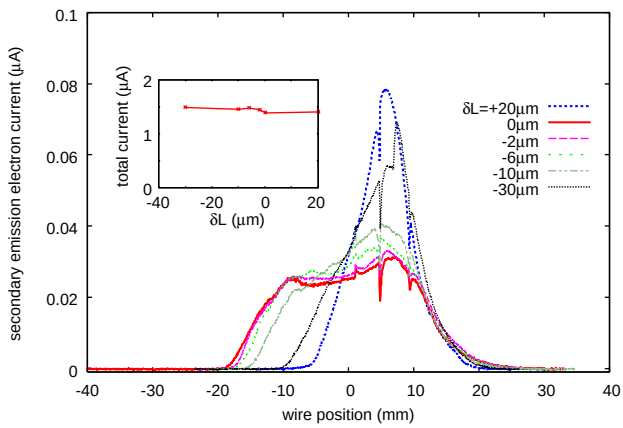

Figure 6: Horizontal beam profiles for various cavity detuning lengths measured with a wire scanner (WIRE #2) placed in the middle of the drift space between two quadrupole magnets just after the second bending magnet in the return arc, where horizontal dispersion should be the same as that of WIRE #1, η = 0.376 m, when the return arc is achromatic. The inset shows the total secondary emission electron current integrated along the wire position with respect to δL.

A drawback of a triple bend achromatic arc is that quadrupole magnets have to be properly set not only to adjust M_{56} for energy compression, but also to establish achromaticity in the arc. This is in contrast to the Bates type end loop where a pair of quadrupole magnets and a pair of sextupole magnets are used just to control M_{56}, T_{566}, respectively, since the end loop is intrinsically achromatic [5]. Therefore achromaticity has to be carefully checked in a triple bend achromatic arc. We have measured horizontal beam profiles downstream of the second bending magnet in the return arc with a wire scanner (see Fig. 6). This wire scanner is called WIRE #2 in the present paper and has been installed in the middle of the drift space between two quadrupole magnets after the second bending magnet and should have the same dispersion function as WIRE #1 when the return arc is achromatic. However, the beam profiles shown in Fig. 6 are similar to those in Fig. 2 only when the FEL efficiency is less than 1%, and they are quite different from each other when the efficiency is higher than 1%, requiring chromaticity correction. The total secondary electron current measured with WIRE #2, which is shown in the inset of Fig. 6, is almost the same as that with WIRE #1. The beam loss is thus expected to be small in the return arc. In the measurement shown in Fig. 6, sextupole magnets are not used to compensate second order aberrations T_{166}, T_{266}, T_{566} arising from the large energy spread due to the FEL interaction. We will perform a systematic measurement of the horizontal beam profiles with various parameter sets of sextupole magents soon.

A current transformer placed downstream of the return arc, which picks up an induction current, is also used as a beam loss monitor for the return arc. The current transformer signal remains almost the same when the FEL efficiency is low, but some beam loss is observed for the efficiency higher than 2%. The beam dump current with respect to δL should be constant when the full energy recovery is established. However the beam current gradually drops as the efficiency increases over 2%, as shown in the inset of Fig. 3. One possible reason is that the energy spread of the recovered beam is beyond the energy acceptance of the beam dump. Although the dump can collect the beam with four times different momentum, the energy spread of the recovered beam can exceed the acceptance under high-efficiency FEL oscillation. Without sufficient energy spread compression, the energy spread can remain 2.5 MeV, which corresponds to 15% of 17 MeV beam, while the mean energy of the recovered beam is lower than 2.5 MeV. We need to study carefully how much beam is recovered through the main SCA modules and how much of the recovered beam is collected by the beam dump.

MAGNETIC BUNCH COMPRESSION IN THE FIRST ARC

A high peak current electron beam, which can be accomplished by means of magnetic, ballistic, or velocity bunch compression, is indispensable to realize a high-efficiency

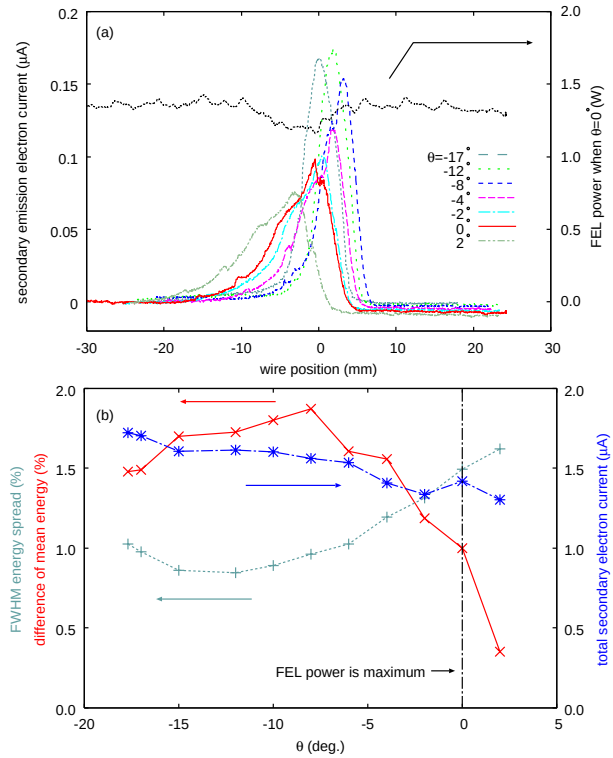

Figure 7: The top figure (a) shows horizontal beam profiles measured with a wire scanner placed just after the first bending magnet in the first arc, where horizontal dispersion is calculated as η = 0.50 m, with respect to the RF phase of the last SCA module M2 defined as θ. The black dotted line shows measured FEL power during a wire scan when $\theta = 0^\circ$, where the FEL power is maximum. The bottom figure (b) shows relative difference of the beam centroid energies (solid line), FWHM energy spreads (dotted line), and the total secondary emission electron current from the wire scanner as a function of θ. Those data are obtained from the top figure (a).

FEL oscillation. At the JAEA ERL, ballistic bunching, which is performed before the main SCA modules, had been considered to play a major role in the bunch compression [25]. Recently we measured powers of coherent synchrotron radiation (CSR) generated from three bending magnets in the first arc and found that the CSR power at the last magnet is much stronger than the remaining two. This indicates that another bunch compression occurs in the first arc. In order to confirm this magnetic bunch compression, we measured horizontal beam profiles with a wire scanner at a dispersive point as a function of the RF phase of the last SCA module (SCA M2). Hereafter we use θ as the RF phase of SCA M2. The horizontal dispersion at the wire scanner located just after the first bending magnet is estimated to be η = 0.50 m from the first-order matrix calculation. The measured beam profiles are shown in Fig. 7(a). Here we set $\theta = 0^\circ$ where the FEL power is maximum. The

black dotted line shows FEL power with respect to the wire position when $\theta = 0°$. The power decreases by 10% when the wire passes the beam centroid. The ratio of FEL power loss is consistent with the ratio of beam loss due to the presence of the wire scanner, which is calculated from the peak secondary current of 0.1 μA divided by the total secondary current of 1.4 μA.

Figure 7(b) shows difference of the mean energy, FWHM energy spread, and total secondary electron current with respect to θ. The energy spread is 1.5% when $\theta = 0°$, but it decreases down to 0.8% as θ decreases to $-12°$. The energy of beam centroid shifts toward higher energy side with decreasing phase and reaches maximum around $\theta = -10°$. The energy difference between $\theta = 0°$ and $\theta = -10°$ is 0.8% corresponding to 0.14 MeV for 17 MeV electron. Since the energy gain for each main SCA module is roughly 7.5 MeV, 11 degree off-crest acceleration yields the same amount of energy difference. From these results, we can conclude that $\theta = 0°$ is about 10 degree off-crest of the SCA M2 phase. The total secondary electron current gradually increases with decreasing θ, and the ratio of the current increases by 20% when $\theta = -17°$. The similar amount of beam loss is observed in another experiment. We have measured beam currents with a Faraday cup both in the straight section along the main SCAs and after the first arc, and observed that the beam loss through the first arc amounts to roughly 20% when the RF phase is adjusted for the FEL power to become maximum. This indicates that the lower energy side of the electron beam arising from the off-crest acceleration is lost at the beam duct of the first bending magnet in the first arc. We have a plan to replace the beam duct with one having larger bore and repeat the same measurement to study the energy spectra of the accelerated electron beam with respect to θ in more details.

We have also measured temporal beam profiles at the undulator center as a function of θ with a synchroscan streak camera (M1954-10, Hamamatsu) at macropulse length of 30 μs, as shown in Fig. 8(a). The centroid of beam profiles changes as a function of θ, since the beam arrival time shifts due to M_{56} from the SCA M2 to the undulator. The shift of arrival time and rms bunch length are shown in Fig. 8(b). The shortest FWHM bunch length of 12 ps is obtained when $\theta = 0°$, indicating that high peak current is indispensable for the high-efficiency FEL oscillation. The arrival time difference between $\theta = 0°$ and $\theta = -10°$ is 10 ps, and the corresponding momentum difference between the two acceleration phases is 0.8% from Fig. 7(b). This leads to M_{56} = 0.38 m, where the sign of M_{56} is determined from first-order matrix calculation of the first arc based on the magnet parameters used for actual operation. The calculation yields M_{56} = 0.6 for the first arc and M_{56} = 0.07 for the half chicane.

We will perform the same measurement somewhere downstream of the second arc to obtain M_{56} from the undulator center to the entrance to the main SCA modules. The value of M_{56} in the return arc should be the same as that to

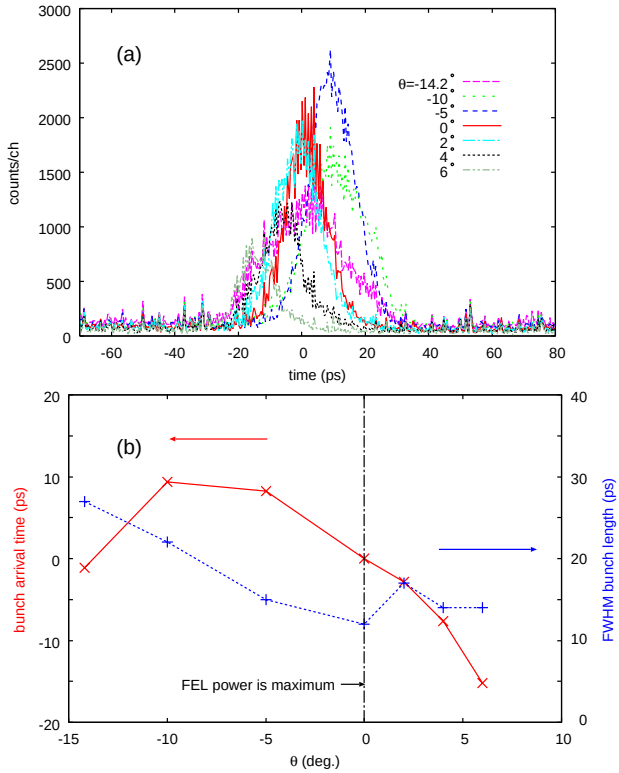

Figure 8: The top figure (a) shows temporal beam profiles measured with a synchroscan streak camera at the undulator center with respect to the RF phase of the SCA M2 (θ). The bottom figure (b) shows relative difference of the beam arrival time (solid line), and FWHM bunch length (dotted line). Those data are obtained from the top figure (a).

the undulator from the exit of SCA M2 except for its sign, if the energy compression in the return arc is properly executed. It is worth to mention that such a longitudinal phase space manipulation using magnetic bunch compression and decompression is performed in JLab FEL in an elegant way [5], where $M_{56} = -0.3$ m from the exit of SCA modules to the undulator for the bunch compression and M_{56} = 0.3 m from the undulator to the entrance of SCA modules for the energy compression.

APPLICATION

A laser-beam transport line has been built to deliver FEL pulses to an experiment room. We have upgraded an optical beam expander, which consists of two elliptic mirrors, at the end of FEL optical cavity to convert a diverging beam from a center-hole on a FEL cavity mirror into a parallel beam. The expanded beam is transported to the experimental room through a 24 m-long evacuated pipe. FEL transport efficiency 50% has been achieved [1].

For FEL applications, we investigate material processing using ultrashort FEL pulses. By using FEL pulse shorter than pico-second, it is possible to avoid thermally induced

stress and debris generation, which has been unavoidable in material processing with Q-switched YAG lasers or CO2 lasers [26]. Recently we found that non-thermal surface peeling of stainless steel by ultrashort laser pulses can be adopted to eliminate stress-corrosion-cracking (SCC), which is a critical problem in nuclear power plants [27]. A pilot experiment using Ti:sapphire laser showed that we can remove the residual stress and SCC susceptibility of cold-worked and hardened stainless steel by the laser peeling. Application of self-chirped FEL pulses is also studied. We reported that frequency chirp is induced in an FEL pulse, when the FEL oscillator has large gain and is operated at perfectly synchronized cavity length [28]. We demonstrated generation of an FEL pulse with frequency chirp of 14% and duration of 320 fs. A laser pulse with such large frequency chirp can be used for quantum control of chemical reaction: the resonant excitation of atomic or molecular systems, which have an anharmonic potential ladder [29].

REFERENCES

[1] H. Iijima et al.," Development of frequency-resolved optical gating for measurement of correlation between time and frequency of chirped FEL", in these proceedings.

[2] S. Benson et al.,"High power lasing in the IR Upgrade FEL at Jefferson Lab", Prof of the FEL-2004, 229 (2004).

[3] S. Benson,"Design challenges in high power free-electron laser oscillators", abstract of the FEL-2005, (2005).

[4] G.R. Neil et al.,"The JLab high power ERL light source", NIM A **557**, 9 (2006).

[5] D. Douglas,"The Jefferson Lab 1kW IR FEL", Prof of the LINAC-2000, 716 (2000).

[6] R. Hajima et al.,"First demonstration of energy-recovery operation in the JAERI superconducting linac for a high-power free-electron laser", NIM A **507**, 115 (2003).

[7] R. Hajima, E.J. Minehara,"Electron beam dynamics through a return-arc and a deceleration path of the JAERI energy-recovery linac", NIM A **507**, 141 (2003).

[8] R. Nagai et al.,"Beam current doubling of JAEA ERL-FEL", in these proceedings.

[9] N. Nishimori et al.,"High extraction efficiency observed at the JAERI free-electron laser", NIM A **475**, 266 (2001).

[10] R. Hajima et al.,"Design of energy-recovery transport for the JAERI FEL driven by a superconducting linac", NIM A **445**, 384 (2000); T. Shizuma et al.,"Simulated performance of the energy-recovery transport system for JAERI-FEL", *ibid* **475**, 569 (2001).

[11] N. Nishimori et al.,"20.8 MHz electron gun system for an energy recovery linac FEL at JAERI", Proc. of the APAC-2004, 625 (2004).

[12] V.P. Bolotin et al.,"Status of the Novosibirsk energy recovery linac", NIM A **557**, 23 (2006).

[13] M. Sawamura et al., "Status and development for the JAERI ERL-FEL for high-power and long-pulse operation", Prof of the EPAC-2004, 1723 (2004); Masaru Sawamura and Ryoji Nagai, "Status of RF system for the JAERI energy-recovery linac FEL", NIM A **557**, 287 (2006).

[14] R. Nagai et al.,"Improvement of RF low-level controller for JAERI ERL-FEL", Prof of the 1st annual meeting of Part. Acc. Soc. of Japan, 293 (2004) (in Japanese).

[15] R. Nagai et al., "Optical resonator optimization of JAERI ERL-FEL", NIM A **528**, 231 (2004).

[16] P. Chevtsov et al., "Non-invasive energy spread monitoring for the JLAB experimental program via synchrotron light interferometers", NIM A **557**, 324 (2006).

[17] A.P. Freyberger and G.A. Krafft, "Summary report on synchronization, diagnostics and instrumentation", NIM A **557**, 370 (2006).

[18] A.P. Freyberger, "Large dynamic range beam profile measurements", Proc of the DIPAC-2005, 12 (2005).

[19] T.I. Smith et al., "Status of the SCA-FEL", NIM A **296**, 33 (1990).

[20] W.A. Gillespie et al.,"Time-resolved electron spectrum measurement on the FELIX facility", NIM A **331**, 786 (1993).

[21] R.I. Cutler et al., "Performance of wire scanner beam profile monitors to determine the emittance and position of high power CW electron beams of the NBS-Los Alamos racetrack microtron", Proc of the PAC-1987, 625 (1987); M.A. Wilson et al., "Performance of the 5 MeV injector for the NBS-Los Alamos racetrack microtron", *ibid*, 322 (1987); D.B. Barlow et al.,"Prototype flying-wire beam-profile monitor", Proc of the PAC-1993, 2480 (1993).

[22] J. Camas et al.,"Observation of thermal effects on the LEP wire scanners", Proc of the PAC-1995, 2649 (1995).

[23] http://www.physics.nist.gov/PhysRefData/Star/Text/contents.html

[24] R. Hajima et al.,"Analyses of superradiance and spiking-mode lasing observed at JAERI-FEL", NIM A **475**, 270 (2001).

[25] R. Hajima et al.,"Development of an energy-recovery linac for a high-power FEL at JAERI", Proc. of the APAC-2004, 245 (2004).

[26] A. Nishimura et al., "Demonstration of material processing using JAERI-FEL", Proc of the FEL-2003, II-57 (2003).

[27] E.J. Minehara et al., "Preparation femtosecond laser prevention for the cold-worked stress corrosion crackings on reactor grade low carbon stainless steel", Prof of the FEL-2004, 665 (2004); E.J. Minehara et al., "JAERI 10kW high power ERL-FEL and its applications in nuclear energy industries", Prof of the FEL-2005, 305 (2005).

[28] Ryoichi Hajima and Ryoji Nagai, "Generation of a self-chirped few-cycle optical pulse in a FEL oscillator", PRL **91**, 024801 (2003).

[29] S. Chelkowski et al.,"Efficient molecular dissociation by a chirped ultrashort infrared laser pulse", PRL **65**, 2355 (1990).